Application of Electrohydrodynamic Atomisation to Surface Disinfection

Arianna Parisi, Domenico Flagiello, Amodio Piscitelli, Francesco Di Natale*

Università di Napoli Federico II, Dipartimento di Ingegneria Chimica, dei Materiali e della Produzione Industriale, Piazzale V. Tecchio 80, 80125 Napoli, Italy
francesco.dinatale@unina.it

The development of improved methods for surface disinfection has gained renewed interest during the first waves of the SARS-COV2 Pandemic when the need to assure massive disinfection of objects and spaces goes against that of reducing the consumption of chemicals and minimize the impact of disinfectants on exposed persons. Electrohydrodynamic atomization is considered a valuable option to improve disinfection efficiency, thanks to the benefits associated with the droplets charge. This paper presents preliminary experimental and model results on the application of an induction charging electrohydrodynamic atomisation process to the spraying of water solution of a conventional disinfectant under model conditions. In particular, electrospraying under simple jet mode with a whipping breakup has been tested. Experiments are aimed to characterize the droplet size distribution, the energy requirements and the spray coverage area over a target surface, while a simplified physical mathematical model is used to estimate the amount of disinfectant lost upon evaporation and the distribution of the droplets over the target surface. The electrospray is able to disperse droplets having a charge-to-mass ratio of around 1.67 mC/kg with an energy consumption of 23.4±7.8 J/L, being more efficient than other conventional hydraulic nozzles. These preliminary findings indicate a good matching between modelled and experimental data and suggest that electrospraying under simple jet mode with a whipping breakup can be a possible option for the spraying of disinfectants over surfaces.

1. Introduction

Surface disinfection is one of the most common practices to contain the spreading of pathologies and has gained significant importance during the first waves of the SARS-COV2 Pandemic. The need to assure massive disinfection of objects and spaces goes against the need to reduce the consumption of chemicals and minimize the impact of disinfectants on exposed persons. Indeed, the chemicals conventionally used as disinfectants are associated with several adverse effects on humans and when they are sprayed over surfaces, proper ventilation of the ambient is needed to assure that their concentration in the air (both in terms of evaporated gases and dispersed aerosols) remains below certain safety limits aimed to prevent acute and chronic exposure risks. The spreading of aerosols and their evaporation in the ambient strongly depend on the physical-chemical properties of the liquid disinfectant and the aerosolization process. Several chemicals have been proposed and accepted for the disinfection of surfaces: ethanol, hydrogen peroxide, chlorine, sodium hypochlorite, quaternary ammonium salts and many others. The specific toxicity for humans of these compounds and their tendency to evaporate and degrade over time, define the constraints for their actual use in disinfection, depending on the specific application (surface or airborne pathogens removal), characteristics of the ventilation systems, and time required before persons can safely enter the disinfected ambient.

Besides, the droplet size and the concentration of the disinfectant achieved on the target surface are critical to assure proper cleaning and minimum consumption of chemicals.

For the elimination of surface pathogens droplets between 10 and 100 μm are usually preferred (e.g., Wood et al., 2021). As a general rule, finer droplets give better coverage and are also effective against airborne pathogens, but, for the same reason, they require a longer time to settle, and appropriate aeration of the

environment is required to reduce inhalation. Besides, they can be easily entrained in air currents. On the other hand, large droplets settle rapidly and are more stable but provide less effective coverage of the surface.

Electrohydrodynamic atomization (EHDA), carried out using electrospray units, is an interesting technique to produce droplets of different sizes, from tenths to hundreds of microns, which bear a net electric charge. The EHDA is based on coupling conventional hydraulic/aerodynamic spraying techniques with the application of electric fields. The energy consumption related to the electric field application is much less than the energy consumption associated with liquid pressurization or with air compression required to provide similar droplet size distributions. However, the effects of EHDA on droplet size and properties are relevant. Droplets produced by EHDA are characterized by faster heat and mass transfer rates, are better dispersed, thanks to the electrostatic repulsion arising from their charges and are better collected over a surface, thanks to the electrostatic attractive forces exerted toward grounded objects. Besides, thanks to the contribution to jet instability induced by the electric field, EHDA allows producing fine droplets without imparting high kinetic energy to the jet, so the droplets rapidly approach terminal velocity and are likely to impact the target surface at lower velocities. These lower impact velocities and the same electric forces between charged droplets and grounded surfaces improve their adhesion, making the drops less prone to inertial rebounding (Deng and Gomez, 2011; Tian et al., 2022; Xu et al., 2021).

These features make EHDA an intriguing method to spray disinfectants by assuring a better distribution of the liquid droplets over the target surface and a lower dispersion of aerosol particles in the surrounding environment. EHDA disinfection has been recently reviewed for very fine droplet sprays, showing the potentialities but also the limits of the process (Wood et al., 2021).

This paper presents preliminary experimental and model results on the application of an induction charging EHDA process to the spraying of water solution of sodium hypochlorite under model conditions. With the target of spraying droplets in the size range of 10-100 μm with a flow rate of some tens of ml/min, simple jet mode with a whipping breakup appears as a promising EHDA technique. Sodium hypochlorite has been chosen because is one of the cheapest and most effective disinfectants and because, as a salt, its evaporation is slower than alcohols or hydrogen peroxides. A physical mathematical model is used to estimate the amount of disinfectant lost upon evaporation of charged droplets and to estimate the concentration of disinfectant which reaches the target surface and its possible coverage. Preliminary experiments are aimed to characterize the droplet size distribution, the atomization energy and the spray coverage area under the experimental conditions.

2. Materials and methods

The electrosprayed liquid was an aqueous solution containing 0.1% w/w NaClO prepared by dilution of a 15% v/v NaClO solution with tap water (conductivity 600 µS/cm, surface tension 0.073 N/m).

Figure 1 reports an assembly of the experimental setup used for the tests.

The experiments were carried out with an electrospray assembly (1) that was built following the same drawings of D'Addio et al. (2014). The electrospray consisted of a stainless-steel capillary needle (OD = 0.8 mm, ID = 0.5 mm) coaxial to a steel ring encased in a PTFE box acting as the charging electrode. The needle tip was located 10 mm below the ring's lower surface, following a nozzle-to-ring-up configuration. The liquid was fed into the needle using a flow-controlled syringe pump (8) operated at a flow rate of 10 ml/min, whose internal calibration was periodically off-line checked by using an in-line rotameter (Yokogawa RAGK series). The syringe pump was chosen both to assure precise and constant dosage of the liquid and to minimize disturbances that amplify the jet breakup mechanisms.

The assembly was supported by a metallic bar with insulating clamps (6) placed over a grounded horizontal surface (11). During these experiments, the ring was connected to the high-voltage generator (9) and the needle acted as the grounded counter-electrode. The setup included systems to provide a direct measurement of droplet size distribution and dispersion current.

The electrospray dispersion current included spray current and parasite gas-discharge currents and was measured at the grounded electrode line with the electrometer (10). Together with the applied potential read at the generator, the dispersion current provided a measurement of the energy consumption of the electrospray. The dispersion current was measured by placing a Keithley mod.6514 electrometer positioned along the electric line connecting the ring electrode with the ground line.

The needle tip was kept 100 mm above a sample substrate (3), which was a wide, flat, smooth horizontal polymeric plate blocked over a moving sledge (4) controlled by an electric brushless motor that moves along a linear path with a velocity up to 100 mm/s. The sledge was placed over an insulating support (6). Preliminary sessile drop measures of the contact angle between the liquid solution and the polymeric substrate used in these tests indicated a value of 70±2° for uncharged droplets. To date, this information is not available for charged droplets.

The in-flight droplet size distribution was analysed by optical methods. These were determined by a Miro C110 high-speed camera equipped with a 100 X microscopic lens and a backlight (THOR LABS, M450LP1) (2). The image files were transferred to a PC and analysed offline (7).
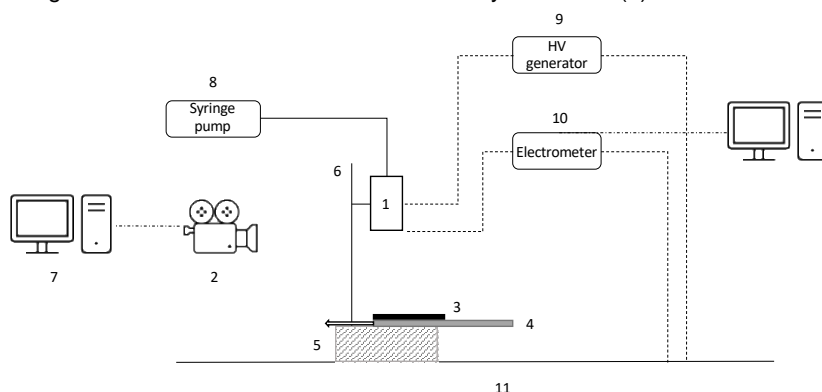

Figure 1 – Scheme of the experimental set-up. 1. Electrospray assembly; 2. Optical system; 3. Sample substrate; 4. Moving sledge (leftward in the Figure); 5. Insulator; 6, Electrospray assembly support; 7. Optical system data recording; 8. Syringe pump; 9. HV direct current generator; 10. Electrometer; 11. Ground

The electrospray was operated in still, open air, and after stabilization, the sample substrate (an opaque polymeric plate) was passed below the spray at a velocity of 80 mm/s to collect the footprint of the sprayed droplets. The liquid spreading over the sample substrate was analysed by acquiring images with an optical microscope (Optika Microscope C-B5).

The images of the electrosprayed droplets and the wet surface were analysed with the software ImageJ®. The droplet size distribution was calculated with Microsoft Excel®. ImageJ internal routines were used to determine the surface area visibly covered by the droplets. It is worth mentioning that droplets finer than 40-50 µm are likely to produce "wet and dry fogs" that cannot be visualised by the optical methods adopted here. ImageJ ® provides sizes of the droplets on the view plane, in terms of the smallest and the largest Feret diameters, *a* and *b*; the droplets either appear as a sphere or as ellipsoids. In both cases, it was assumed that droplets were prolate spheroids, having the third axis equal to the smaller one of those visible on the view plane, i.e., *a*. The droplet Sauter diameter, *d*, was thus calculated for each droplet and the spray size distribution was determined using Microsoft Excel®.

The needle was operated at a potential of 13 kV, which corresponded to whipping breakup conditions. The establishment of whipping breakup mode can be observed through the optical analysis of the jet and from the observation of the droplet average size distribution.

A simple droplet dynamics model was used to estimate the droplet trajectories, their evaporation and the relative concentration of the solute reaching the surface. The evaporation model was developed based on the Abramzon and Sirignano (1989) equations for a single droplet modified according to Combe and Donaldson (2017) to account for the presence of sodium hypochlorite. Under this simplified model solution, the speciation of sodium chlorite was neglected, and it was assumed that all the salt remains undissolved in water. The model included a simplified analysis of droplets dynamics, which were assumed to leave the jet at the same velocity as the liquid at the needle tip, accomplishing their terminal velocity after a stopping distance which was calculated according to the classical textbooks of Hinds (2010) and Seinfeld and Pandis (1998).

The pertinent literature indicates that the presence of electric charge over water droplets allows decreasing the evaporation rate, thanks to the improved tendency to attract dipolar water molecules in the gas phase (Reznikov et al., 2016; Salazar et al., 2015). This result is consistent with the results on SO_2 absorption by charged droplets both at the laboratory scale (Di Natale et al., 2016, 2018, 2019) and pilot scale (Di Natale et al., 2022) and has a beneficial effect on surface disinfection processes, because lower evaporation means less reduction of droplets size and lower risk to disperse them as a consequence of the air motion in the surrounding environment. Although these effects should be included in the evaporation model, at the moment there is still a lack of mathematical models to account for the presence of electric charge at the interface of a liquid mixture drop. Therefore, in this work, we considered a more restrictive condition assuming that charged droplets evaporate exactly as they are not charged.

Besides, it is also known that droplets emitted by electrospray are characterised by an evident deformation, because of surface charge distribution and of their interference with the surrounding electric field (related to the jet, the electrodes, the surrounding surface and the same remaining droplets). However, under the whipping

conditions investigated therein, most of the sprayed droplets were finer than 100 μm and in this case, they reached a spherical shape soon, while the larger ones appeared heavily deformed and oscillating. The characteristics of this droplet's motion need further analysis, and in this work, the classical Frossling equations for gas-film mass and heat transfer of spherical isolated droplets were adopted.

$$Sh = 2 + 0.552Re^{1/2}Sc^{1/3} \tag{1}$$

$$Nu = 2 + 0.552Re^{1/2}Pr^{1/3} \tag{2}$$

Where Sh, Nu, Re, Sc and Pr are, respectively, the Sherwood and the Nusselt numbers of the droplets, the Reynolds number, the Schmidt number, and the Prandtl number referred to droplet Sauter diameter and gas phase properties. The model consists of a system of mixed algebraic and ordinary differential equations that were solved numerically using MATLAB®. The model was applied to single droplets having diameters representative of the size distribution function determined by the experiments.

3. Results and discussion

Figure 2 shows the probability density function, PDF, of the droplet Sauter's diameters determined for the electrospray unit operated under a 10 mL/min flow rate, and 13 kV of applied voltage. Three curves are reported therein: the droplets population has been weighted in terms of number distribution, surface area distribution and volume distribution.
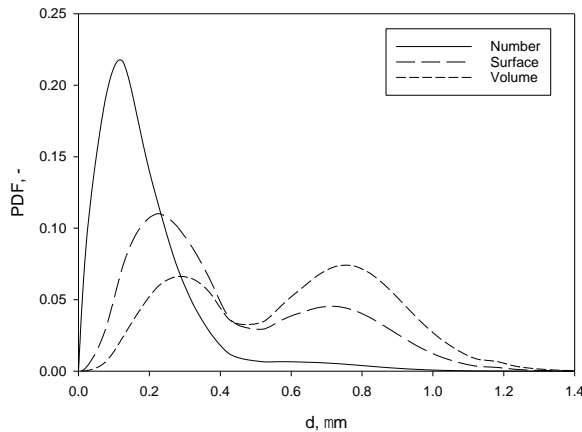

Figure 2 – Probability density function for the sprayed droplet size at 13 kV 10 mL/min.

In terms of number distribution, the size distribution was consistent with former findings for distillate water (Agostinho et al., 2018) and showed a mean value of nearly 120 μm and a standard deviation of 100 μm. While this distribution showed a dominant single mode, the surface and volume distributions, as well as the optical analysis, showed the existence of two droplet populations, which can be well described by Gaussian functions. The fine droplets population was characterized by a surface and volume mean and standard deviation of 230±115 μm and 290±120 μm, respectively while the corresponding means and standard deviations for the coarse droplets' population were respectively of 720±190 μm and 760±200 μm.
The fine population was by far dominant in terms of the number concentration of sprayed droplets, but the coarse population was more than half of the sprayed mass and about one-third of the surface area of the sprayed droplets. Most of the droplets belonging to the finer fraction had a spherical shape, while the larger ones were instead deformed, with higher deformation levels closer to the liquid jet breakup point.
Figure 3a shows an example of surface coverage achieved after around 1 s of the passage of the sample substrate below the spray. The optical analysis reveals an overall coverage of 13%. It is worth noticing that we measured the visible wet area instead of the overall coverage, and that with this technique it was hard to detect with due precision isolated droplets deposits finer than 100 μm. Of course, isolated wet or dry fog droplets were not detected at all. Besides, it was also impossible to distinguish between liquid deposits deriving from single coarse population droplets or coalescence of fine and coarse droplets. As a consequence, the wet-covered area is expected to be a little lower than the one actually covered by the spray.
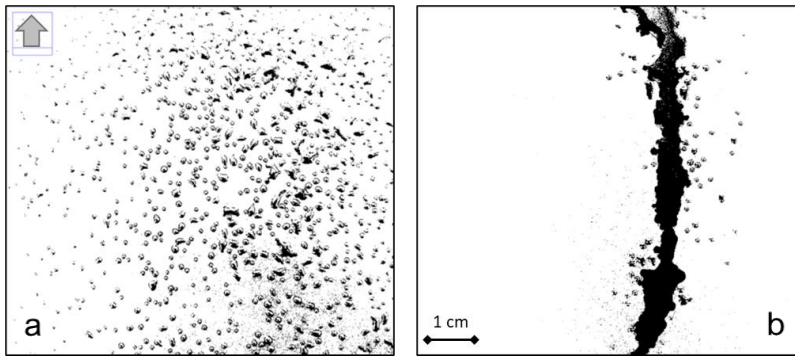
Figure 3 – Sprayed droplets dispersed over a portion of the sample substrate. a: 13 kV 10 mL/min; b: 0 kV 10 mL/min. Substrate moving at 80 mm/s following the trajectory indicated by the arrow at the top left corner.

Under these premises, it is clear that the most visible deposits appear as large elements, mostly related to the coarse population of the sprayed droplet distribution and to coalescence phenomena, so that the average surface size distribution of the deposited droplets corresponded to 1470 ± 220 µm. However, several smaller objects having a size below 200 µm appeared. Assuming the average contact angle of 70±2° determined from the sessile drop experiments, this corresponded to an average sprayed droplet size of nearly 950 µm. This is larger than the average droplet size of the coarse population mode, but consistent with the possibility of coalescence phenomena and with the possible reduction of surface tension (and thus of contact angle) expected for charged droplets. As a reference, to attribute this average deposited size of 1470 µm to the average size of the coarse population fraction (around 760 µm volumetric mean) a 45° of contact angle is needed. Unfortunately, at this stage, this possible increase of liquid spreading as a consequence of the reduced surface tension is not yet verifiable from experiments. As a mere comparison, Figure 3b shows the surface coverage achieved by the same spray units operated at 0 kV, as a simple jet, not electrified spray. The comparison clearly highlights how the spray properties dramatical change in the presence of an electric field since, although the amount of water dispersed over the substrate is identical, the coverage is very different because of the spreading conditions. As aforementioned, the coalescence of droplets is likely to take place over the substrate, but despite this effect, the coverage is much higher for the electrified spray than for the uncharged one. Figure 4 shows the results of droplet evaporation for three reference droplet sizes, covering the fine population of the droplet size distribution function.
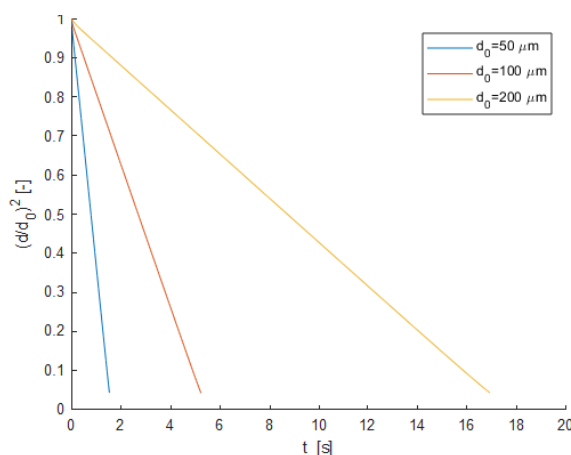

Figure 4. Droplet evaporation model results. The parameter d/d_0 indicates the ratio between the droplet size at time t, d, and the initial droplet size, d_0.

These are plotted in terms of the ratio between the actual and the initial droplet size, which, assuming a spherical shape, corresponds to the ratio between the square of the actual and the initial droplet Sauter diameters. When compared with the time required to reach the target substrate placed 100 mm below the spray, this corresponds to evaporation of 1.8% of the total sprayed volume. The sodium hypochlorite concentration proportionally increases.

Besides, considering the actual droplet evaporation, knowing the average spray angle (around 48°) and assuming the contact angle of 45° for charged water solution, we estimated a theoretical surface coverage achieved by the electrospray of 16.5% of the spotted area, which is higher but consistent with the one observed in the experiments. Finally, an estimation of energy consumption for the electrospray unit can be easily achieved from the mean value of the dispersion current at the applied potential, whose average value resulted as low as 0.3±0.1 μA. At the applied potential of 13 kV, this corresponds, indeed, to an energy requirement of 23.4±7.8 J/L. These are typical energy consumptions for similar electrospray units and Agostinho et al. (2018) already demonstrated that these systems are almost twice as efficient as a pressure swirl atomizer operated at 10 MPa overpressure required to produce similar droplets size.

4. Conclusion

Electrohydrodynamic atomization is emerging as a valuable tool to improve the spreading of disinfectants over contaminated surfaces thanks to the better adhesion and dispersion of charged droplets and the fine-tuning of droplet size distribution. This work explores the possible use of electrospray in whipping mode to distribute an aqueous solution of sodium hypochlorite 0.1% w/w over a surface to simulate a disinfection process. The experiments reveal that the whipping mode can produce droplets in a desirable size range for disinfection sprays, although a bimodal distribution function is achieved. The spray is capable of providing an even distribution of the liquid over a surface, despite the ubiquitous presence of coalescence phenomena. The energy requirement is 23.4±7.8 J/L, being more efficient than other conventional hydraulic nozzles. This finding suggests that the use of electrospray in whipping mode can be a valid option for surface disinfection and further pursuits will be dedicated to this subject in the next future.

References

Abramzon, B., Sirignano, W.A., 1989. Droplet vaporization model for spray combustion calculations, International Journal of heat and Mass Transfer, 32(9), 1609-1618

Agostinho, L.L.F., Bos, B., Kamau, A., Brouwer, S.P., Fuchs, E.C., Marijnissen, J.C.M., 2018. Simple-jet mode electrosprays with water. Description, characterization and application in a single effect evaporation chamber. J Aerosol Sci 125, 237–250.

Combe, N.A., Donaldson, D.J., 2017. Water Evaporation from Acoustically Levitated Aqueous Solution Droplets. Journal of Physical Chemistry A 121, 7197–7204.

D'Addio, L., Carotenuto, C., Balachandran, W., Lancia, A., di Natale, F., 2014. Experimental analysis on the capture of submicron particles (PM0.5) by wet electrostatic scrubbing. Chem Eng Sci 106.

D'Addio, L., Di Natale, F., Carotenuto, C., Balachandran, W., Lancia, A., 2013. A lab-scale system to study submicron particles removal in wet electrostatic scrubbers. Chem Eng Sci 97, 176–185.

Deng, W., Gomez, A., 2011. Electrospray cooling for microelectronics. Int J Heat Mass Transf 54, 2270–2275.

Di Natale, F., Carotenuto, C., Caserta, S., Troiano, M., Manna, L., Lancia, A., 2019. Experimental evidence on the chemi-electro-hydrodynamic absorption of sulphur dioxide in electrified water sprays. Chemical Engineering Research and Design 146, 249–262.

Di Natale, F., Carotenuto, C., Lancia, A., 2016. Enhanced SO2 removal by using charged water droplets. Chem Eng Trans 52, 505–510.

Di Natale, F., Carotenuto, C., Manna, L., Lancia, A., 2018. Chemi-electro-hydrodynamic of sulphur dioxide absorption by electrified water sprays. Chem Eng Trans 69, 685–690.

Di Natale, F., Carotenuto, C., Parisi, A., Flagiello, D., Lancia, A., 2022. Wet electrostatic scrubbing for flue gas treatment. Fuel 325, 124888.

Hinds, W.C., Kennedy, N.J., 2010. Aerosol Science and Technology John Wiley & Sons, Inc., New York.

Reznikov, M., Salazar, M., Page, M., Rivera-Sustache, M., 2016. Further Progress in the Electrostatic Nucleation of Water Vapor, Proc. of the 2016 Electrostatic Joint Conference. Purdue University, p. B2.

Salazar, M., Minakata, K., Reznikov, M., 2015. Electrically Enhanced Condensation II: Effects of the Electrospray. IEEE Trans Ind Appl 51, 1146–1152.

Seinfeld, J.H., Pandis, S.N., 1998. Atmospheric Chemistry and Physics, from Air Pollution to Climate Change. John Wiley & Sons, Inc., New York.

Tian, Y., Wang, H., Zhou, X., Xie, Z., Zhu, X., Chen, R., Ding, Y., Liao, Q., 2022. How does the electric field make a droplet exhibit the ejection and rebound behaviour on a superhydrophobic surface? J Fl. Mech 941.

Wood, J.P., Magnuson, M., Touati, A., Gilberry, J., Sawyer, J., Chamberlain, T., McDonald, S., Hook, D., 2021. Evaluation of electrostatic sprayers and foggers for the application of disinfectants in the era of SARS-CoV-2. PLoS One 16.

Xu, H., Wang, J., Li, B., Yu, K., Tian, J., Wang, D., Zhang, W., 2021. Effect of spray modes on electrospray cooling heat transfer of ethanol. Appl Therm Eng 189.